Structure of FAD-Bound L-Aspartate Oxidase: Insight into Substrate Specificity and Catalysis[†,‡]

Roberto T. Bossi,[§,||] Armando Negri,[⊥] Gabriella Tedeschi,[⊥] and Andrea Mattevi*[,§]

Dipartimento di Genetica e Microbiologia, Università di Pavia, via Abbiategrasso 207, 27100 Pavia, Italy, DISCAFF, Università del Piemonte Orientale "Amedeo Avogadro", viale Ferrucci 33, 28100 Novara, Italy, and Dipartimento di Patologia Animale, Igiene e Sanità Pubblica, Università di Milano, via Celoria 10, 20133 Milano, Italy

Received November 13, 2001; Revised Manuscript Received December 19, 2001

ABSTRACT: L-Aspartate oxidase (Laspo) catalyzes the conversion of L-Asp to iminoaspartate, the first step in the de novo biosynthesis of NAD^+. This bacterial pathway represents a potential drug target since it is absent in mammals. The Laspo R386L mutant was crystallized in the FAD-bound catalytically competent form and its three-dimensional structure determined at 2.5 Å resolution in both the native state and in complex with succinate. Comparison of the R386L holoprotein with the wild-type apoenzyme [Mattevi, A., Tedeschi, G., Bacchella, L., Coda, A., Negri, A., and Ronchi, S. (1999) *Structure 7*, 745−756] reveals that cofactor incorporation leads to the ordering of two polypeptide segments (residues 44−53 and 104−141) and to a 27° rotation of the capping domain. This motion results in the formation of the active site cavity, located at the interface between the capping domain and the FAD-binding domain. The structure of the succinate complex indicates that the cavity surface is decorated by two clusters of H-bond donors that anchor the ligand carboxylates. Moreover, Glu121, which is strictly conserved among Laspo sequences, is positioned to interact with the L-Asp α-amino group. The architecture of the active site of the Laspo holoenzyme is remarkably similar to that of respiratory fumarate reductases, providing strong evidence for a common mechanism of catalysis in Laspo and flavoproteins of the succinate dehydrogenase/fumarate reductase family. This implies that Laspo is mechanistically distinct from other flavin-dependent amino acid oxidases, such as the prototypical D-amino acid oxidase.

Bacteria are able to synthesize NAD^+ using L-Asp and dihydroxyacetone phosphate as precursors (*1*). This pathway is absent in mammals and represents an attractive target for drug design studies. The first step in prokaryotic NAD^+ biosynthesis is carried out by L-aspartate oxidase (Laspo),[1] which catalyzes the conversion of L-Asp to iminoaspartate (Figure 1) (*2*). In the course of this reaction, the essential FAD cofactor oxidizes the substrate and is subsequently reoxidized by molecular oxygen to produce hydrogen peroxide. The enzyme is also able to utilize fumarate as an electron acceptor, yielding succinate. The ability to use both oxygen and fumarate in cofactor reoxidation is physiologically relevant in that it enables Laspo to be functional under both aerobic and anaerobic conditions (*3*, *4*).

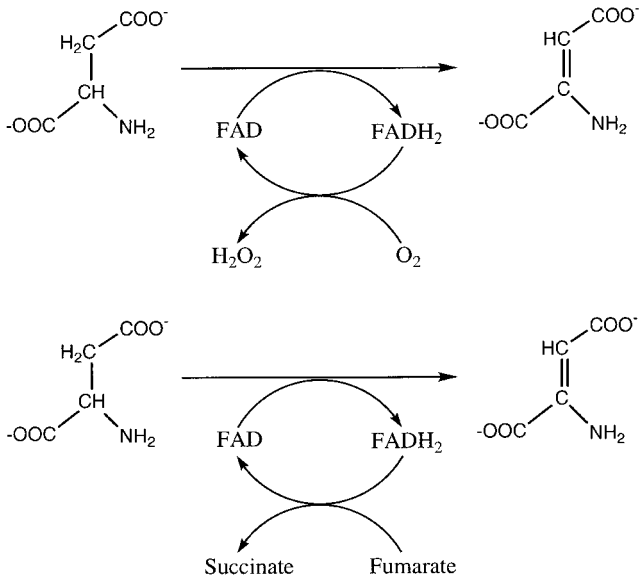

FIGURE 1: Scheme of the reaction catalyzed by Laspo. The enzyme is able to use as electron acceptors for FAD reoxidation both molecular oxygen and fumarate. The reaction product is represented in the amine form.

Laspo is member of the succinate dehydrogenase/fumarate reductase family of flavoproteins (*5*−*7*) which includes

[†] This research was supported by grants from Consiglio Nazionale delle Ricerche of Italy (target-oriented project on biotechnology), Agenzia Spaziale Italiana, and Ministero della Università e Ricerca Scientifica e Tecnologica.

[‡] Atomic coordinates and structure factors have been deposited in the Protein Data Bank (*32*) as entries 1KNR and r1KNRsf for native R386L Laspo and 1KNP and r1KNPsf for R386L in complex with succinate.

* To whom correspondence should be addressed: Dipartimento di Genetica e Microbiologia, Università di Pavia, via Abbiategrasso 207, 27100 Pavia, Italy. Phone: +39-0382-505560. Fax: +39-0382-528496. E-mail: mattevi@ipvgen.unipv.it.

[§] Università di Pavia.

[||] Università del Piemonte Orientale "Amedeo Avogadro".

[⊥] Università di Milano.

[1] Abbreviations: Laspo, L-aspartate oxidase; FAD, flavin adenine dinucleotide; rmsd, root-mean-square deviation; FRD, fumarate reductase; FC3, flavocytochrome c_3; PDB, Protein Data Bank; Hepes, *N*-(2-hydroxyethyl)piperazine-*N*′-2-ethanesulfonic acid; Tris, tris(hydroxymethyl)aminomethane.

10.1021/bi015939r CCC: $22.00
Published on Web 02/08/2002

flavocytochrome c_3 (FC3) and the flavoprotein subunit of the membrane-bound succinate dehydrogenase and fumarate reductase (FRD). These oxidoreductases share several functional properties, all acting on dicarboxylic substrates. However, Laspo is unique in that it is unable to oxidize succinate. The low (−216 mV) redox potential of the Laspo-bound FAD cofactor is thought to represent a thermodynamic barrier that prevents succinate oxidation (*4*).

Alignment of the amino acid sequences of members of the succinate dehydrogenase/fumarate reductase family reveals considerable homology with ∼30% sequence identity. The recent determination of the crystal structures of two membrane-bound FRDs (*6*, *8*), FC3 (*9*) and Laspo (*5*), has highlighted their clear structural homology. In all these enzymes, the FAD cofactor is bound to a FAD-binding domain, exhibiting the Rossmann fold topology. The active center is lined with several strictly conserved amino acids, including three Arg and two His side chains.

The recombinant wild-type Laspo from *Escherichia coli* was crystallized in the apo form (*5*). The structure revealed the overall architecture of the protein, although the absence of the cofactor prevented the analysis of the enzyme in a catalytically active conformation. All attempts to crystallize the wild-type protein in the holo form were unsuccessful. The R386L mutant, in which an active site Arg is replaced with Leu (*10*), turned out to be amenable to crystallization in the active FAD-bound state, producing a new crystal form. The resulting holoenzyme structure reveals the basis of the substrate specificity and provides strong evidence for the notion that Laspo functions through a mechanism that is distinct from that of other flavin-dependent amino acid oxidases.

EXPERIMENTAL PROCEDURES

Materials. Sodium citrate, sodium succinate, glycerol, 2-propanol, *N*-(2-hydroxyethyl)piperazine-*N*′-2-ethanesulfonic acid (Hepes), tris(hydroxymethyl)aminomethane (Tris), sodium dodecyl sulfate, 2-mercaptoethanol, phenylmethanesulfonyl fluoride, and soybean trypsin inhibitor were from Sigma. Trypsin was from Boehringer Mannheim (Mannheim, Germany).

Crystallization and Data Collection. The R386L mutant of *E. coli* Laspo was purified as described previously (*10*). Attempts to crystallize the mutant by means of the protocol employed for the wild-type protein (*5*) failed. A screening of conditions using commercially available kits (Hampton Research) led to the discovery that yellow regularly shaped bipyramidal crystals could be obtained using 2-propanol as the precipitant. Refinement of these conditions resulted in an optimized protocol for crystallization of the R386L mutant. Crystals were obtained by the vapor diffusion method at 22 °C. The well solutions consisted of 100 mM Hepes/KOH (pH 7.5), 100 mM sodium citrate (pH 7.5), and 4−8% (v/v) 2-propanol. Hanging drops were formed by mixing equal volumes of 50 mg/mL protein in 50 mM Hepes/KOH (pH 8.0) and well solutions. Crystals appeared after a few days and reached a maximum size of 0.1 mm × 0.1 mm × 0.2 mm. They were also obtained in the presence of 10 mM sodium succinate. Attempts to crystallize the wild-type protein following this protocol were unsuccessful.

Diffraction data were measured at beamline ID14-EH2 of the European Synchrotron Radiation Facility (Grenoble, France) using a MarCCD detector. Before data collection, crystals were washed for a few seconds in a cryoprotectant solution consisting of 100 mM Hepes/KOH (pH 7.5), 100 mM sodium citrate (pH 7.5), 10% (v/v) 2-propanol, 20% (v/v) glycerol, and, when required, 10 mM sodium succinate. Even if data were measured at 100 K, the data collection experiments were severely hampered by the very high level of radiation damage exhibited by the crystals. Data processing and reduction were carried out using MOSFLM (*11*) and programs of the CCP4 suite (*12*). The crystals belong to space group $P4_12_12$ with one Laspo monomer in the asymmetric unit and the following unit cell parameters: $a = b = 72$ Å and $c = 310$ Å. Complete data sets were measured to 2.5 Å resolution using one crystal of the native protein and to 2.6 Å from two crystals of the succinate complex. Data collection statistics are reported in Table 1.

Table 1: Data Collection and Refinement Statistics

	cocrystallized with succinate	native
resolution (Å)	2.6	2.5
space group	$P4_12_12$	$P4_12_12$
cell dimensions *a* and *c* (Å)	72.54, 309.12	73.28, 313.93
no. of crystals	2	1
no. of observations	100758	68503
no. of unique reflections	22099	26873
completeness (%)[a]	94.3 (91.9)	96.1 (96.4)
R_{sym} (%)[a,b]	11.6 (37.7)	10.7 (37.3)
no. of protein atoms	4150	4150
no. of waters	21	25
no. of FAD atoms	53	53
no. of ligand atoms	8	−
R_{factor} (%)[c]	23.2	24.8
R_{free}	28.1	29.5
rmsd for bond lengths (Å)[d]	0.025	0.022
rmsd for bond angles (deg)[d]	2.5	2.6
Ramachandran analysis[e]		
most favored (%)	84	82
additionally allowed (%)	16	18

[a] The values for the highest-resolution shell are in parentheses. [b] $R_{sym} = \sum_h\sum_i|I_i(h) - I(h)|/\sum_h\sum_i I_i(h)$, where $I_i(h)$ and $I(h)$ are the *i*th and mean measurements of reflection *h*, respectively. [c] *R*-factor $= \sum_h||F_o| - |F_c||/\sum_h|F_o|$, where F_o and F_c are the observed and calculated structure factors of reflection *h*, respectively. [d] The rmsds from the ideal values were calculated with the program Refmac (*15*). [e] Calculated with Procheck (*17*).

Structure Solution and Refinement. The structure of the R386L Laspo mutant was determined by molecular replacement using the program Amore (*13*) and the native data set. Various search models were tested. A clear solution was obtained using a "modified" wild-type apoenzyme model (PDB entry 1CHU). This was constructed by moving the capping domain into the same orientation observed in the *Shewanella fridigimarina* FC3 structure (*9*). The correctly oriented and translated model was subjected to rigid body refinement. The resulting electron density map clearly indicated the presence of bound FAD and of an ordered conformation for stretches of the polypeptide chain that are disordered in the apoenzyme. Model building was carried out with the program O (*14*). The model was refined using the maximum likelihood refinement program Refmac version 5 (*15*). All measured data (no σ cutoff) were employed. Ordered water molecules were automatically added using Arp (*16*). The refined native atomic coordinates provided the starting model for the refinement of the succinate complex, using the same methodology that was employed for the native

structure. The set of reflections for R_{free} calculation was identical to that of the native structure refinement. The quality of the stereochemical parameters was evaluated with the program Procheck (*17*). A summary of refinement statistics is presented in Table 1.

Analysis and inspection of the three-dimensional structures were carried out with O (*14*) and programs of the CCP4 package (*12*). Cavities were calculated with the program Voidoo (*18*) using a probe radius of 1.4 Å. Cutoff distances of 4.0 and 3.4 Å were used for van der Waals contacts and H-bonds, respectively. Figures were generated with Ligplot (*19*), Molscript (*20*), and Bobscript (*21*).

Limited Proteolysis of the R386L Mutant. The R386L mutant was incubated in 50 mM Hepes/KOH (pH 8.0) in the presence of 10% (w/v) sequence-grade trypsin. FAD (1 mM) was included in the incubation mixture. At different times, aliquots (8 μg) were diluted 3-fold in 125 mM Tris-HCl (pH 6.8), 4% (w/v) sodium dodecyl sulfate, 1.42 mM 2-mercaptoethanol, 2 mM phenylmethanesulfonyl fluoride, and soybean trypsin inhibitor (10/1, w/w with respect to protease). Samples were immediately incubated at 100 °C for 5−10 min and subjected to SDS−PAGE electrophoretic analysis (*22*). Gels were stained for protein content with Coomassie Blue R-250. Densitometric measurements of the stained gels were taken at 630 nm with a Bio-Rad model GS-700 laser densitometer interfaced with a Hewlett-Packard computer. N-Terminal sequencing was performed on polyvinylidene difluoride electrotransferred samples using an automated protein sequencer (model 477A, Applied Biosystems, Foster City, CA).

RESULTS

Overall Structure and FAD Binding. Crystals of the R386L mutant of *E. coli* Laspo grew under different conditions and displayed different symmetry with respect to the wild-type apoenzyme. The mutant was crystallized using 2-propanol as the precipitant. The bright yellow color of the R386L crystals indicated the presence of bound FAD in the crystalline protein. Crystals were grown in both the presence and absence of succinate, a reaction product when fumarate is the electron acceptor (Figure 1). The structure was determined by molecular replacement using the wild-type model (PDB entry 1CHU). The atomic coordinates for the succinate complex were refined to a final *R*-factor of 23.2% (R_{free} = 28.1%) at 2.6 Å resolution, while coordinates of the native protein were refined to a final *R*-factor of 24.8% (R_{free} = 29.5%) at 2.5 Å resolution (Table 1). In both structures, the FAD cofactor is well-defined by the electron density map (Figure 2). The native and succinate-containing structures are virtually identical in both overall conformation and active center geometry, with a root-mean-square deviation (rmsd) of 0.26 Å for 529 Cα atoms (0.35 Å for all 4150 protein atoms). For the analysis of the model, we shall mainly refer to the structure resulting from cocrystallization with succinate.

The structure of holo Laspo consists of three domains (Figure 3): the FAD-binding domain (residues 5−243 and 349−410) with the classic dinucleotide binding fold observed in many flavoproteins (*23*), the capping domain (residues 244−348) with an irregular α+β topology, and the helical C-terminal domain (residues 411−533). Such a three-domain architecture is identical to that observed in the apoprotein (*5*) and in the flavoprotein subunit of the membrane-bound FRD (*6*, *8*). The FAD is bound in an elongated conformation to the FAD-binding domain, with no cofactor atoms being solvent accessible. The binding site displays the typical features of the dinucleotide binding fold (Figure 4) (*23*, *24*).

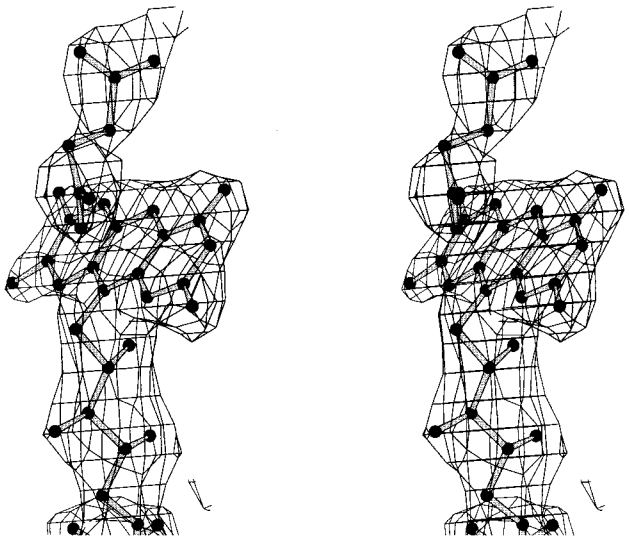

FIGURE 2: Stereodiagram of the final electron density for FAD and succinate. The map was computed with σA-weighted coefficients using the final model and contoured at the 1σ level. Produced with Bobscript (*21*).

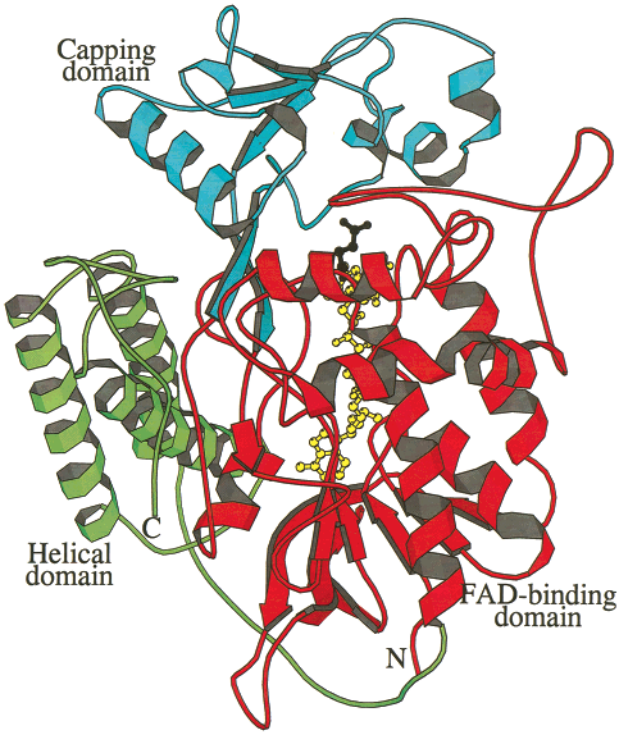

FIGURE 3: Structure of *E. coli* Laspo in the FAD-bound holo form. The FAD-binding domain is in red, the C-terminal domain in green, and the capping domain in cyan. The N-terminal and C-terminal amino acids of the model are labeled with the letters N and C, respectively. The tight association between the capping domain and the FAD-binding domain is apparent from the ribbon diagram. The FAD and succinate ligands are in yellow and black, respectively. The orientation is the same as in Figure 2. Produced with Molscript (*20*).

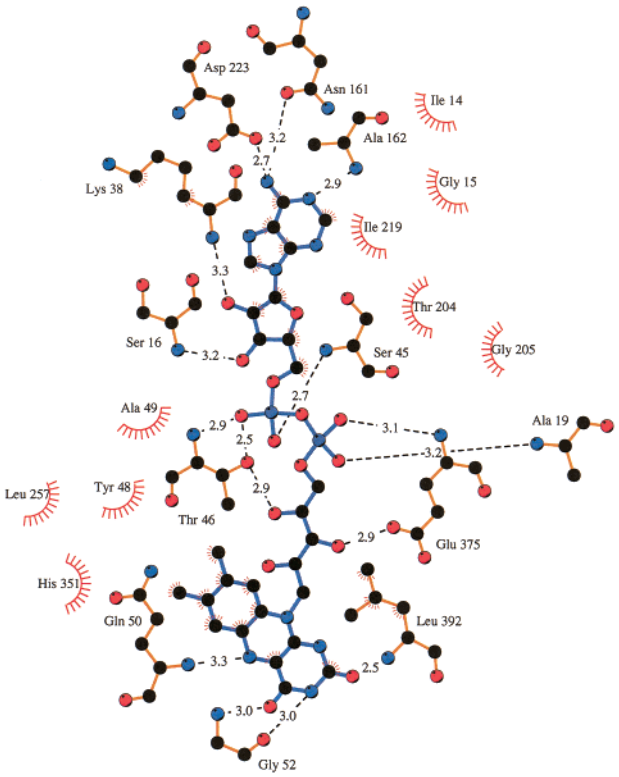

FIGURE 4: Ligplot (*19*) schematic illustration of Laspo residues interacting with FAD. H-Bonds are outlined with dashed lines. Distances are in angstroms. Carbon atoms are in black, oxygen atoms in red, phosphorus atoms in violet, and nitrogen atoms in blue.

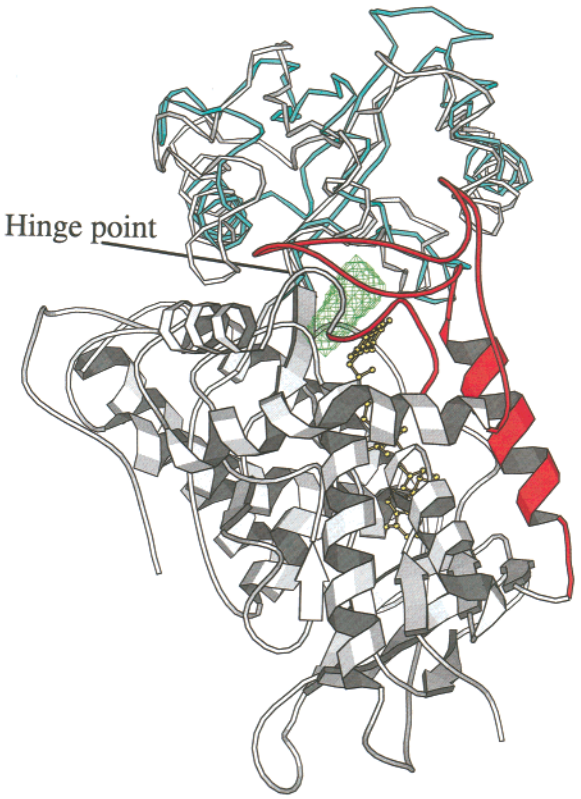

FIGURE 5: Rotation (27°) of the capping domain. The drawing was generated by superimposing the residues of the FAD-binding domain and C-terminal domain of the apo wild-type Laspo structure (PDB entry 1CHU) onto the holoprotein. The holoenzyme is in gray with the two segments (residues 44−53 and 104−141) that become ordered upon cofactor incorporation outlined by the red color. The capping domain of the superimposed apo structure is shown as a cyan ribbon, highlighting the difference in the orientation. Specifically, the capping domain of the holoprotein adopts a closed conformation that defines the interdomain substrate cavity (shown in green chicken-wire representation). The FAD is in yellow. The hinge point formed by residues Phe243, His244, and Pro348 is denoted. With respect to Figure 2, the model has been rotated by 40° around an axis vertical in the plane of the paper. Produced with Bobscript (*21*).

The pyrophosphate negative charges interact with the N-terminal residues of two helical segments (residues 18−28 and 45−48); the adenine ring is H-bonded to an amino acid (Ala162) of a β-strand belonging to the so-called β-meander, and the 3′-OH group of the ribityl chain is H-bonded to a side chain carboxylate (Glu375). The isoalloxazine ring adopts a planar conformation (Figure 2) and is located on the side of the FAD-binding domain facing the capping domain (Figure 3). The flavin N1−C2═O2 locus is in contact with the first amino acid (Leu392) of the C-terminal helix (residues 392−409) of the FAD-binding domain. An additional key element for flavin binding is the loop of residues 49−57. The cofactor N5 atom interacts with the backbone nitrogen of Gln50, while the N3 and O4 atoms are H-bonded to the O and N atoms of Gly52, respectively.

Active Site. The active site of Laspo is formed by a cavity (Figure 5), which has a volume of 110 Å^3 and is lined by the isoalloxazine ring and amino acids of both the capping domain (His244, Leu257, Leu258, Thr259, Glu260, Ser261, and Arg290) and the FAD-binding domain (Gln50, Gly51, Gly52, Glu121, His351, Leu386, Ser389, Ser391, and Leu392). The architecture of the substrate-binding site can be analyzed with reference to the structure of the complex with succinate, which is well-defined by the electron density (Figure 2). The residues lining the active site effectively shield succinate, which is totally solvent inaccessible when bound in the active site cavity. The ligand is anchored to the protein by interactions established by its two carboxylate groups (Figure 6). The oxygen atoms of the C1 carboxylate (the atomic numbering is described in Figure 6) are within hydrogen bonding distance of the side chains of His244 and Thr259 and the main chain nitrogens of Gly51 and Glu260. The C4 carboxylate group points toward Leu386 and is H-bonded to the side chain of His351 and the backbone N atom of Ser389. The succinate carbon skeleton is sandwiched between the Arg290 and Glu121 side chains and the flavin ring. The C2 and C3 methylene groups are 3.4 and 3.0 Å from the flavin N5 and Arg290 NH2 atoms, respectively. The presence of such unusual contact between a carbon of the active site ligand and Arg290 guanidinium side chain has been also observed in the structures of FC3 (*9*) and FRD (*25*) and has profound mechanistic implications (see below).

Biochemical characterization of the R386L mutant has shown that the amino acid replacement severely impairs catalysis, inducing a 2000-fold decrease in K_{cat} and a 700-fold increase in K_m (*10*). The three-dimensional structure of the mutant holo form reveals a binding mode of succinate consistent with a key role of the side chain at position 386. Indeed, the structure strongly indicates that in the wild-type Laspo, the Arg386 guanidinum moiety most likely interacts with the ligand carboxylate, in the same way as observed in FC3 (*9*) and FRD (*8*). Thus, the effect of the R386L mutation on the enzyme activity seems primarily due to the removal

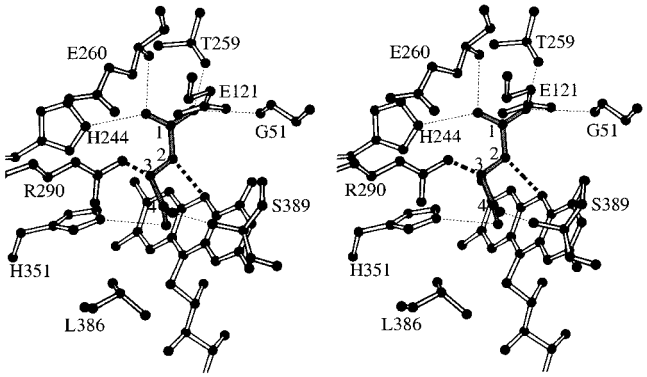

FIGURE 6: Stereodiagram of the succinate-binding site. The ligand is outlined by gray bonds. H-Bonds are represented by thin dashed lines. The thick dashed lines indicate the contacts between the succinate C2 and C3 atoms with flavin N5 and Arg290 (3.4 and 3.0 Å, respectively). The atomic numbering of succinate is identical to that used for fumarate in FC3 structures (*31*). C1 is on the carboxylate that interacts with Gly51, His244, Thr259, and Glu260. C2 is the methylene carbon in contact with flavin N5. C3 is the methylene in contact with Arg290. The C4 carboxylate interacts with His351, Ser389, and Leu386.

from the active center of a crucial element for substrate binding and charge compensation.

The conformation of the active site residues in the R386L protein crystallized in the absence of active site ligands (native structure in Table 1) is identical to that of the succinate-bound protein, the cavity being occupied by ordered water molecules. In addition, a strong electron density peak in the active site has been interpreted as being due to a Cl^- ion, which binds in the same position occupied by the C1 carboxylate of succinate.

Limited Proteolysis of the R386L Mutant. The structure of the R386L mutant was also probed by limited proteolysis. The time course of limited trypsin digestion followed by SDS−PAGE analysis showed that the holo form of the R386L mutant undergoes a complete degradation in smaller fragments. The major proteolytic products obtained upon tryptic digestion were isolated by SDS−PAGE, electroblotted, and subjected to N-terminal sequencing to identify the sites of cleavage. The results show that the proteolysis pattern is identical to the one previously described for the Laspo wild-type protein (*22*). The same results were obtained in the presence of 10 mM succinate, L-Asp, and fumarate. This supports the contention that the R386L mutation does not cause large conformational changes with respect to the wild-type holoprotein.

Comparison between the Holo and Apo Forms. Knowledge of the structures of the FAD-free wild-type protein and of the FAD-bound R386L mutant allows a comparison between the Laspo holo and apo forms. Binding of FAD appears to be associated with considerable changes in FAD-binding domain tertiary structure as well as the mutual orientation of the domains forming the enzyme. Superposition of the residues forming the closely assembled FAD-binding domain and C-terminal domain (Figure 3) results in an rmsd of 1.0 Å for the 343 Cα atoms that are ordered in both structures (residues 5−40, 60−100, 150−240, 350−410, and 420−533). These residues are left essentially unaltered by cofactor incorporation, the largest variation being an ≈1 Å shift of residues 217−220, which are close (though not in direct contact with) to the cofactor ribose. The main effect of FAD binding is the ordering of two long polypeptide stretches (residues 44−53 and 104−141; Figure 5) that are disordered in the apoprotein. The loop of residues 44−53 protrudes from the FAD-binding domain (Figure 5), forming a niche for isoalloxazine binding. The segment of residues 104−141 consists of a long loop (residues 104−135) followed by an α-helix (residues 136−150). These residues contribute to the sealing of the active site cavity and take part in substrate binding through the Glu121 side chain (Figure 6). The ordering of these two polypeptide segments is remarkable in that it involves a total of 46 amino acids, corresponding to 15% of the residues (residues 1−243 and 349−410) forming the FAD-binding domain.

Another major difference between the apo and holo structures concerns the capping domain. Analysis by the program DynDom (*26*) shows that this domain is differently oriented by 27° with respect to the FAD-binding domain. The rotation is of the hinge type and does not significantly affect the domain conformation as indicated by an rmsd of 0.48 Å for 105 Cα atoms in the capping domain of the holo and apo structures. The hinge point is formed by Phe243, His244, and Pro348, which belong to the linkers connecting the capping domain to the FAD-binding domain. The main consequence of the hinge motion is the formation of the active site cavity with the closure of the wide interdomain cleft present in the apoprotein (Figure 5).

The closed conformation of the holo structure enables a tight association between the capping domain and the FAD-binding domain with formation of interdomain H-bonds and van der Waals contacts. Many of these involve residues 119−127, belonging to one of the two segments that are disordered in the apoprotein. Clearly, domain closure and ordering of residues 44−51 and 104−141 are not independent phenomena. Cofactor incorporation seems to be necessary to fix the conformation of residues forming the flavin- and substrate-binding site, which may in turn favor closing of the capping domain. Thus, cofactor binding in Laspo is a combination of preorganization and induced fit; the bulk of the FAD site is preorganized in the apoprotein, but some polypeptide segments attain a defined conformation only in the presence of the cofactor. In this respect, the mechanism of flavinylation in Laspo partly differs from that of vanillyl alcohol oxidase, in which FAD binds with a lock-and-key mechanism to a highly complementary and preorganized cofactor binding site present in the apoenzyme (*27*).

Comparison with Fumarate Reductases. The three-dimensional structures of other members of the succinate dehydrogenase/fumarate reductase family are known. These include the membrane-bound FRDs from *E. coli* (*6*) and *Wolinella succinogenes* (*8*, *25*) and flavocytochrome c_3, a soluble homologue of FRD, from *S. frigidimarina* (*9*) and *Shewanella putrefaciens* (*28*). For a comparison with the Laspo holoenzyme, we have referred to the structures of enzyme complexes with dicarboxylate ligands: FC3 from *S. frigidimarina* in complex with a malate-like molecule (determined at 1.8 Å resolution; PDB entry 1QJD) and the flavoprotein subunit of *W. succinogenes* FRD in complex with fumarate (2.2 Å; PDB entry 1QLB) and malonate (3.1 Å; PDB entry 1E7P).

The FRD complexes with fumarate and malonate differ by a 14° rotation of the capping domain, which in the fumarate-bound protein adopts a "half-closed" conformation

while in the malonate complex is in a "closed" position. Comparison of the individual domains of Laspo with the malonate-bound FRD shows that the residues forming the FAD-binding domain and C-terminal domain superimpose with an rmsd of 1.5 Å (336 Cα atoms), whereas the capping domain gives an rmsd of 1.3 Å (94 Cα atoms). These calculations also indicate that the capping domain of the FRD−malonate complex is only slightly rotated (4°) with respect to Laspo, proving that the closed conformation of the malonate-bound FRD is essentially identical to that of the Laspo holoenzyme. A high level of structural similarity also emerges from the comparison with FC3−ligand complex. FC3 lacks the C-terminal domain, which is replaced by an N-terminal heme domain (*9*). The FAD-binding domain and the capping domain of FC3 superimpose onto those of Laspo with rmsds of 1.4 Å (241 Cα atoms) and 0.6 Å (48 Cα atoms), respectively. Moreover, the capping domain is rotated by only 5° with respect Laspo, implying that also in the case of FC3 the orientation of the capping domain is identical to that of the Laspo holoprotein.

The presence of the same orientation of the capping domain in the Laspo holoenzyme, FC3, and malonate-bound FRD is reflected in a remarkable similarity in the active site geometry (Figure 7a,b). Specifically, in Laspo and FC3, the ligand C1 and C4 carboxylates are held in position by interactions with two conserved clusters of H-bond donors. Likewise, the C2 carbon is in contact with the flavin N5, while C3 interacts with and Arg side chain (Arg290 in Laspo and Arg402 in FC3). Such a high level of conservation supports the notion that the closed position of the capping domain represents the catalytically competent form of the enzyme (*7*).

The only significant difference in the active site of Laspo with respect to the fumarate reductase structures is in the side chain of Glu121, which corresponds to Met236 in FC3 and Phe141 in FRD (Figure 7a,b). Alignment of the amino acid sequences (*7*, *29*) indicates that Glu121 is strictly conserved among Laspo proteins, but it is replaced by aliphatic side chains in succinate dehydrogenases and FRDs. Glu121 lies on the surface of the substrate cavity, in a position that is suited for interaction with the α-amino group of the L-Asp substrate, possibly establishing an H-bond. Thus, this residue appears to be a key structural determinant dictating the specificity of Laspo for the L-Asp substrate (*4*), which cannot be oxidized by FRD and succinate dehydrogenase.

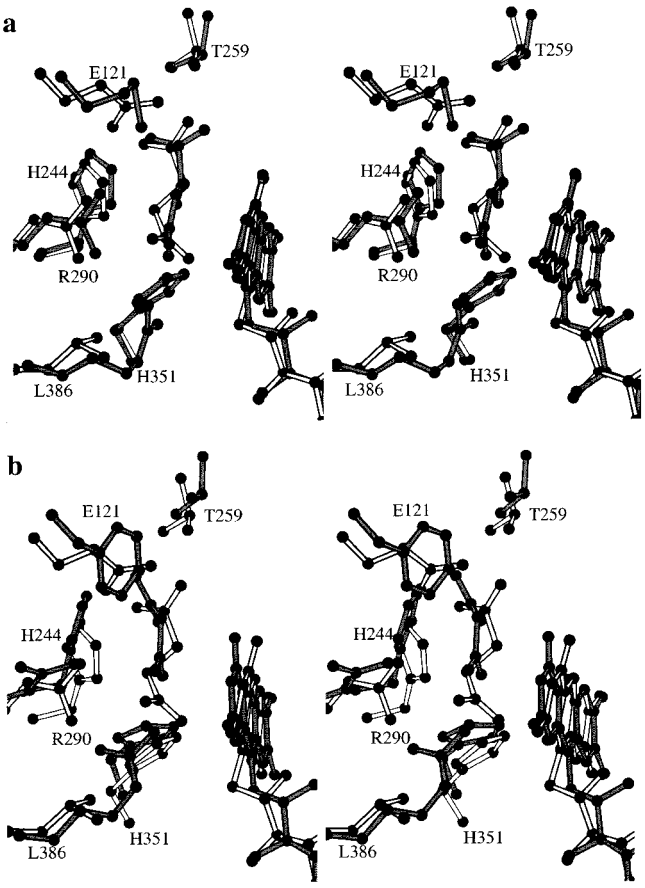

FIGURE 7: Comparison of the active site of R386L Laspo with that of oxidoreductases of the succinate dehydrogenase/fumarate reductase family. The residue numbering of *E. coli* Laspo sequence is used. The only active site residue that is not conserved is Glu121 of Laspo, which corresponds to Met236 of FC3 and Phe141 of FRD. (a) Stereoview of the superposition of the active site of R386L Laspo onto FC3 (gray bonds) in complex with a malate-like molecule (PDB entry 1QJD). (b) Superposition of the R386L active site onto that of the FRD from *W. succinogenes* (gray bonds) in complex with malonate (PDB entry 1E7P). The position of the FRD residue (Arg301) homologous to Laspo Arg290 is tentative since this residue lacks clear electron density in the FRD structure (*25*).

DISCUSSION

Despite a large number of attempts, wild-type Laspo so far has not been crystallized in a cofactor-bound form. The R386L mutation causes a 2-fold reduction in the affinity for FAD, with the K_d value changing from 3.8 μM in the wild type to 8.1 μM in the mutant (*10*). Arg386 is at the interface between the FAD-binding domain and the capping domain and does not take part in crystal contacts in the wild-type apoenzyme crystals. Therefore, crystallization of the R386L mutant in the holo form is surprising and difficult to explain. Replacement of Arg386 with an aliphatic side chain exposes on the active site surface a hydrophobic patch. This may favor closure of the capping domain, making the protein amenable to crystallization in the holo form. Support for this hypothesis derives from the perturbed spectral properties of the R386L mutant, which exhibits a shoulder around 470 nm in its absorption spectrum, indicative of a more hydrophobic flavin environment (*10*).

The Laspo holoprotein exhibits a remarkable similarity to the fumarate reductases of known structure in both overall conformation and active site architecture. A general mechanism shared by the members of the succinate dehydrogenase/fumarate reductase family of oxidoreductases has been proposed (*7*). Fumarate reduction involves hydride transfer from flavin N5 to fumarate C2 coupled to proton donation by an active site residue (Figures 6 and 8). The residue performing acid or base catalysis is the Arg side chain corresponding to Arg290 of Laspo. The structure of the Laspo−succinate complex is in excellent agreement with this mechanistic proposal. The succinate C2 atom is in the expected position for hydride transfer to N5, while C3 is 3.0 Å from Arg290. Such a short contact between the ligand methylene group and the guanidinium nitrogen is consistent with the role of Arg290 in fumarate protonation. Indeed, replacement of this residue with Leu leads to a totally inactive enzyme that, however, fully retains the ability to bind

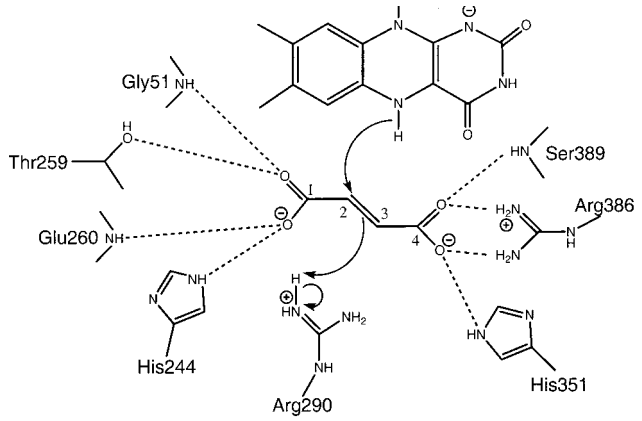

FIGURE 8: Reaction scheme for fumarate reduction by the succinate dehydrogenase/fumarate reductase oxidoreductases with reference to the active site residues of Laspo.

dicarboxylate ligands (*10*). Another key feature of the proposed mechanism is admission of the substrate into a solvent-protected active site. The comparison between the Laspo holo and apo structures highlights the ability of residues linking the capping domain to the FAD-binding domain to act as hinge points. This allows opening and closure of the capping domain, which, therefore, may function in active site gating (Figure 5).

The structure of the holoenzyme identifies Glu121 as the likely side chain involved in binding and recognition of the substrate α-amino group. The L-Asp oxidation reaction can be expected to be the reversal of fumarate reduction (Figure 8). Thus, L-Asp is oxidized through hydride transfer to FAD in conjunction with proton abstraction by Arg290. L-Asp, unlike the fumarate and succinate substrates of FRDs and succinate dehydrogenases, is an asymmetric molecule. The structure of the succinate complex does not allow us to determine whether the atom involved in hydride transfer to the flavin is Cα or Cβ (i.e., which atom binds in the site occupied by succinate C2; see Figures 6 and 8). Solution of this riddle must await further structural and enzymological studies. Nevertheless, it is evident that Laspo functions through a mechanism that differs substantially from that employed by other flavin-dependent amino acid oxidases, such as the prototypical D-amino acid oxidase (*30*). These oxidases act on the Cα NH_2 group, generating the imine form of the substrate. Conversely, the structural data suggest that Laspo acts on the Cα and Cβ atoms, producing the amine form of iminoaspartate (Figure 1). The existence of two mechanisms for flavin-dependent amino acid oxidation underscores the catalytic versatility of the flavin cofactors.

ACKNOWLEDGMENT

We thank M. Rizzi (Università di Pavia) for many helpful suggestions and C. Lina (Università di Pavia) for his initial contribution to the crystallization experiments. The supervision of the ESRF staff during synchrotron data collection is gratefully acknowledged.

REFERENCES

1. Magni, G., Amici, A., Emanuelli, M., and Raffaelli, N. (1999) *Adv. Enzymol. Relat. Areas 73*, 135−183.
2. Nasu, S., Wicks, F. D., and Gholson, R. K. (1982) *J. Biol. Chem. 257*, 626−632.
3. Tedeschi, G., Negri, A., Mortarino, M., Ceciliani, F., Simonic, T., Faotto, L., and Ronchi, S. (1996) *Eur. J. Biochem. 239*, 427−433.
4. Tedeschi, G., Zetta, L., Negri, A., Mortarino, M., Ceciliani, F., and Ronchi, S. (1997) *Biochemistry 36*, 16221−16230.
5. Mattevi, A., Tedeschi, G., Bacchella, L., Coda, A., Negri, A., and Ronchi, S. (1999) *Structure 7*, 745−756.
6. Iverson, T. M., Luna-Chavez, C., Cecchini, G., and Rees D. C. (1999) *Science 284*, 1961−1966.
7. Reid, G. A., Miles, C. S., Moysey, R. K., Pankhurst, K. L., and Chapman, S. K. (2000) *Biochim. Biophys. Acta 15*, 310−315.
8. Lancaster, C. R., Kroger, A., Auer, M., and Michel, H. (1999) *Nature 402*, 377−385.
9. Taylor, P., Pealing, S. L., Reid, G. A., Chapman, S. K., and Walkinshaw, M. D. (1999) *Nat. Struct. Biol. 6*, 1108−1112.
10. Tedeschi, G., Ronchi, S., Simonic, T., Treu, C., Mattevi, A., and Negri, A. (2001) *Biochemistry 40*, 4738−4744.
11. Leslie, A. G. (1999) *Acta Crystallogr. D55*, 1696−1702.
12. Collaborative Computational Project Number 4 (1994) *Acta Crystallogr. D50*, 760−767.
13. Navaza, J. (1994) *Acta Crystallogr. A50*, 157−163.
14. Jones, T. A., Zou, J. Y., Cowan, S. W., and Kjeldgaard, M. (1991) *Acta Crystallogr. A47*, 110−119.
15. Murshudov, G. N., Vagin, A. A., and Dodson, E. J. (1997) *Acta Crystallogr. D53*, 240−255.
16. Lamzin, V., and Wilson, K. S. (1993) *Acta Crystallogr. D49*, 129−147.
17. Laskowski, R. A., MacArthur, M. W., Moss, D. S., and Thornton, J. M. (1993) *J. Appl. Crystallogr. 26*, 283−291.
18. Kleywegt, G. J., and Jones, T. A. (1994) *Acta Crystallogr. D50*, 178−185.
19. Wallace, A. C., Laskowski, R. A., and Thornton, J. M. (1995) *Protein Eng. 8*, 127−134.
20. Kraulis, P. J. (1991) *J. Appl. Crystallogr. 24*, 946−950.
21. Esnouf, R. M. (1999) *Acta Crystallogr. D55*, 938−940.
22. Tedeschi, G., Negri, A., Ceciliani, F., Mattevi, A., and Ronchi, S. (1999) *Eur. J. Biochem. 260*, 896−903.
23. Dym, O., and Eisenberg, D. (2001) *Protein Sci. 10*, 1712−1728.
24. Vallon, O. (2000) *Proteins 38*, 95−114.
25. Lancaster, C. R., Gross, R., and Simon, J. (2001) *Eur. J. Biochem. 268*, 1820−1827.
26. Hayward, S., and Berendsen, H. J. C. (1998) *Proteins 30*, 144−154.
27. Fraaije, M. W., van Den Heuvel, R. H., van Berkel, W. J., and Mattevi, A. (2000) *J. Biol. Chem. 275*, 38654−38658.
28. Leys, D., Tsapin, A. S., Nealson, K. H., Meyer, T. E., Cusanovich, M. A., and Van Beeumen, J. J. (1999) *Nat. Struct. Biol. 6*, 1113−1117.
29. Iverson, T. M., Luna-Chavez, C., Schröder, I., Cecchini, G., and Rees, D. C. (2000) *Curr. Opin. Struct. Biol. 10*, 448−455.
30. Mattevi, A., Vanoni, M. A., and Curti, B. (1997) *Curr. Opin. Struct. Biol. 7*, 804−810.
31. Mowat, C. G., Moysey, R., Miles, C. S., Leys, D., Doherty, M. K., Taylor, P., Walkinshaw, M. D., Reid, G. A., and Chapman, S. K. (2001) *Biochemistry 40*, 12292−12298.
32. Berman, H. M., Westbrook, J., Feng, Z., Gilliland, G., Bhat, T. N., Weissig, H., Shindyalov, I. N., and Bourne, P. E. (2000) *Nucleic Acids Res. 28*, 235−242.

BI015939R